VERSITA

Cent. Eur. J. Chem. • 9(6) • 2011 • 962-971
DOI: 10.2478/s11532-011-0092-9

Central European Journal of **Chemistry**

High Stokes shift long-wavelength energy gap regulated fluorescence in the series of nitro/dimethylamino-substituted ortho-analogs of POPOP

Invited Paper

Rodion Yu. Iliashenko[1], Olexiy S. Zozulia[1], Andrey O. Doroshenko[1,2]

[1]*Kharkov V.N. Karazin National University, Kharkov 61077, Ukraine*

[2]*Ukrainian-American Laboratory of Computational Chemistry, Kharkiv 61001 (Ukraine) and Jackson, Mississippi 38217-0510 (United States)*

Received 24 May 2011; Accepted 18 July 2011

Abstract: A series of novel nitro-substituted *ortho*-analogs of POPOP was synthesized. Like the most of the other known compounds of this class, the synthesized molecules demonstrate high Stokes shift fluorescence emission owing to the planarization of their molecules at electronic excitation. Significant fluorescence quenching in polar solvents was described as the "energy gap law" action rather than the specific effect of the dialkylamino group excited state twisting.

Keywords: *Ortho-analogs of POPOP • High Stokes shift fluorescence • Solvatochromism • Energy gap law • ESS-analysis.*

1. Introduction

The planar and rigid molecular structure is usually considered as the necessary requirement for the synthesis of potentially effective organic fluorescent compounds [1-3]. However, low Stokes shifts, typical of such molecules, in many cases play the role of the limiting factor at their practical application owing to the significant reabsorption effects resulting from the overlap of their absorption and emission spectra, see for example [4-7]. Several photophysical mechanisms were proposed to increase the Stokes shift [8], the most prospective among them seems the effect of the excited state planarization of the initially non-planar fluorescent molecules [9].

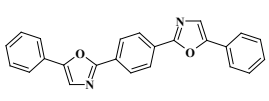

POPOP

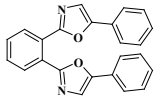

ortho-POPOP

Ortho-analogs of the widely known organic fluorophore POPOP {1,4-bis-(2-phenyl-5-oxazolyl)benzene, which is extensively used in plastic and liquid scintillating compositions [10, 11]} were started in our research group at the early 1990s [12-15]. Bulky substituents in the *ortho*-positions of the central benzene nucleus result in the significantly non-planar molecular structure of *ortho*-POPOPs, that is why these compounds usually absorb light in the lower-wavelength spectral region compared to that of their planar *para*-isomers [14,16]. High Stokes shifts of 9000-10000 cm^{-1} observed in solvents of various polarity and even in the crystalline state were clarified by the definite excited state flattening of their molecules resulting in the restoration of conjugation and in the lowering of the energy of the structurally relaxed excited state [17,18]. Low solvatochromic effects are generally typical of most of the earlier investigated *ortho*-analogs of POPOP owing to the electronic symmetry of their molecules in the structurally relaxed lowest excited singlet state [19,20].

The hypothesis about the possibility of further Stokes shift increase at combination of at least two different photophysical mechanisms in the same molecule mentioned in [8] was formulated in [9] and tested in several of our earlier publications [19,21]. In this paper we try to combine the excited state structural relaxation

* *E-mail: andrey.o.doroshenko@univer.kharkov.ua*

typical to *ortho*-analogs of POPOP with the solvent relaxation around the molecule increasing its dipole moment at electronic excitation.

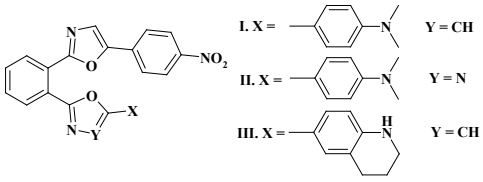

For this purpose, a series of the new *ortho*-analogs of POPOP possessing the effective electron donor and electron acceptor groups was synthesized and characterized by their absorption and emission spectra. Increased intramolecular donor-acceptor interaction in these molecules should result in the significant increase of the excited state polarity introducing the additional solvatochromic contributions to their Stokes shift values in polar media.

2. Experimental procedure

2.1. Chemicals and materials

Solvents and several semi-products were purchased from Aldrich and used without additional purification.

The title compounds were synthesized by the following common scheme:

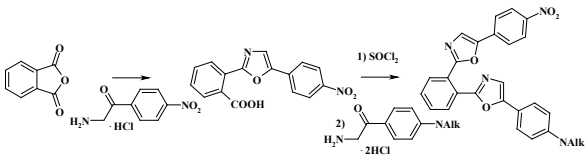

2-(5-[4-nitro-phenyl]-2-oxazolyl)-benzoic acid. 3.7 g (0.025 mol) of phthalic anhydride and 5 g (0.23 mol) ω-amino-4-NO_2-acetophenone hydrochloride were dissolved in 50 mL of dry acetone, then 4 g of potassium carbonate was added in small portions at continuous stirring over 3 hours. At 20 minutes after the addition of the first amount of carbonate, the reaction mixture became viscous.

Then the reaction mass was neutralized by concentrated hydrochloric acid, the yellow solid was filtered off, washed with water and dried.

The obtained amide was dissolved in 50 mL of concentrated sulfuric acid and left to stay in a dark place at room temperature during 12 hours. The reaction mixture was poured on ice, the precipitated solid was filtered, washed with water, dried and doubly recrystallized from toluene to yield 4.96 g (68%) of 2-(5-[4-nitro-phenyl]-2-oxazolyl)-benzoic acid (pale yellow powder, M.P. 168-170ºC).

Carboxylic acid chlorides were synthesized before their subsequent use at boiling of the correspondent acid solution in $SOCl_2$ during 3 hours, than dry toluene was added and the excess of thionyl chloride was removed by distillation.

1-(5-[4-N,N-dimethylamionophenyl]-2-oxazolyl)-2-(5-[4-nitrophenyl]-2-oxazolyl)-benzene (compound **I**). Solution of 1.6 g (0.0048 mol) of 2-(5-[4-nitro-phenyl]-2-oxazolyl)-benzoyl chloride in 25 mL of toluene was mixed with solution of 1.2 g (0.0048 mol) of 4-N,N-dimethylamino-ω-aminoacetophenone dihydrochloride in 50 mL of water. Saturated water solution of sodium carbonate was added dropwise at intensive stirring to pH 9-10, then the reaction mixture was stirred over an hour. Precipitated solid was filtered, washed with water and dried. The obtained arylamide was dissolved in concentrated sulfuric acid at 50-60ºC, then left to stay at room temperature during 5 hours, poured onto ice, neutralized by solid sodium carbonate to pH 8-9, filtered, washed with water and dried. The final product was purified by hot column chromatography on Al_2O_3 with carbon tetrachloride as eluent followed by double recrystallization from octane to yield 0.88 g (0.0019 mol, 49%) of red polycrystalline powder, M.P. 118-119ºC (**$C_{28}H_{20}N_4O_4$**, MW 452.46, molecular ion in MS, *m*/*z*: 452).

1-(5-[4-N,N-dimethylamionophenyl]-1,3,4-oxadiazol-2-yl)-2-(5-[4-nitrophenyl]-2-oxazolyl)-benzene (compound **II**). Mixture of 2 g (0.0065 mol) of 2-(5-[4-nitro-phenyl]-2-oxazolyl)-benzoic acid and 1.2 g (0.0067 mol) of 4-N,N-dimethylaminobenzoic acid hydrazide was boiled in 20 mL of phosphorus oxychloride over 3 hours. The reaction mass was poured into ice and after complete hydrolysis of $POCl_3$, water was added to 1 liter. Precipitated solid was filtered, washed by water to the neutral reaction and dried. The product was purified by hot column chromatography on Al_2O_3 and carbon tetrachloride as eluent and then recrystallized from toluene to yield 1.27 g (0.00028 mol, 43%) of orange crystals, M.P. 146-147ºC ($C_{25}H_{19}N_5O_4$, MW 453.45, molecular ion in MS, *m*/*z*: 453).

ω-amino-1-(1,2,3,4-tetrahydroquinolin-6-yl) ethanone. Quinoline (38.7 g, 0.3 mol), formamide (78 g, 1.65 mol) and 85% formic acid (7.5 g) in 200 mL flask was heated to 175-180ºC on the metal bath during 6 hours, then 2.5 hours – to 190ºC. The reaction mixture was cooled, poured into 750 mL of water and basified by aqueous NaOH. After 3 hours of periodical stirring needed for the decomposition of the excessive formamide the mixture was extracted 4 times by diethyl ether. The ether was removed by distillation, 30 mL of 85% formic acid was added to the dark residue, and the mixture was

boiled under reflux over 30 minutes. Then it was basified and extracted four times by diethyl ether. The extracts were combined, dried under anhydrous sodium sulfate and then ether was removed by distillation in the water bath. The residue was distilled under reduced pressure (10-15 mm Hg). The fraction boiling at 190-200ºC was collected yielding 26 g (0.162 mol, 53%) of yellow liquid, N-formyl-1,2,3,4-tetrahydroquinoline.

20 g (0.124 mol) of N-formyl-1,2,3,4-tetrahydroquinoline, 50 g of anhydrous $AlCl_3$ in 100 mL of methylene chloride was cooled on the ice bath, then 0.15 mol of monochloroacetic acid chloride was added dropwise. The reaction mixture was stirred during 12 hours and then poured on ice. The organic layer was separated, several times washed with 5% hydrochloric acid, and then methylene chloride was removed under reduced pressure. The residue was hydrolyzed at boiling with 50 mL of concentrated hydrochloric acid until homogenization. The mixture was neutralized by solid sodium carbonate, cooled. The yellow crystals of 2-chloro-1-(1,2,3,4-tetrahydroquinolin-6-yl)ethanone was precipitated (16 g, 0.076 mol, 70%).

14 g of the above semi-product (0.069 mol), 10 g of hexamethylenetetramine and 40 mL of chloroform were stirred during 5 hours at room temperature, then white crystals were filtered, washed with cool chloroform and dried. The obtained acylation product was dissolved in 40 mL of 96% ethyl alcohol, 10 mL of concentrated hydrochloric acid was added and the mixture was left at room temperature overnight. The precipitated solid was filtered, some additional amount of the product was collected at partial evaporation of the filtrate at reduced pressure. Finally 7 g (0.027 mol, 66%) of ω-amino-1-(1,2,3,4-tetrahydroquinolin-6-yl)ethanone dihydrochloride with M.P. 246-249 ºC was obtained in such a way.

6-(2-{2-[5-(4-nitrophenyl)-1,3-oxazol-2-yl] phenyl}-1,3-oxazol-5-yl)-1,2,3,4-tetrahydroquinoline (compound **III**). 1.2 g of 2-(5-[4-nitro-phenyl]-2-oxazolyl)-benzoic acid was boiled in 20 mL of phosphorus oxychloride during 1 hour, then 1 g of ω-amino-1-(1,2,3,4-tetrahydroquinolin-6-yl)ethanone dihydrochloride was added and the mixture was additionally boiled up to 3 hours. The reaction mixture was cooled, poured into ice and neutralized by saturated aqueous sodium carbonate. Precipitated solid was filtered, washed with water and dried. The product was purified by hot column chromatography on silica gel and benzene as eluent, then the room temperature column chromatography was applied (silica gel – benzene + 1% triethylamine mixture) to yield 0.5 g (0.0011 mol, 28%) of red crystals with M.P. 102-103ºC ($\mathbf{C_{27}H_{20}N_4O_4}$, MW 464.47, molecular ion in MS, *m*/*z*: 464).

Purity of all the synthesized fluorescent compounds was checked by TLC (Silufol UV-254) and confirmed additionally by the single-banded fluorescence synchronous scan spectra in octane, recorded with $\Delta\lambda_{EX/EM}$ = 50 nm. No normal Stokes shift emitting components were registered for the case of $\Delta\lambda_{EX/EM}$ = 10 nm.

2.2. Spectra measurement

Electron impact (70 eV) mass-spectra were determined on a Varian 1200L device.

Electronic absorption spectra were recorded on a UV/Vis spectrophotometer Hitachi U3210, fluorescence spectra and quantum yields – on fluorescence spectrometer Hitachi F4010 in the standard 1 cm

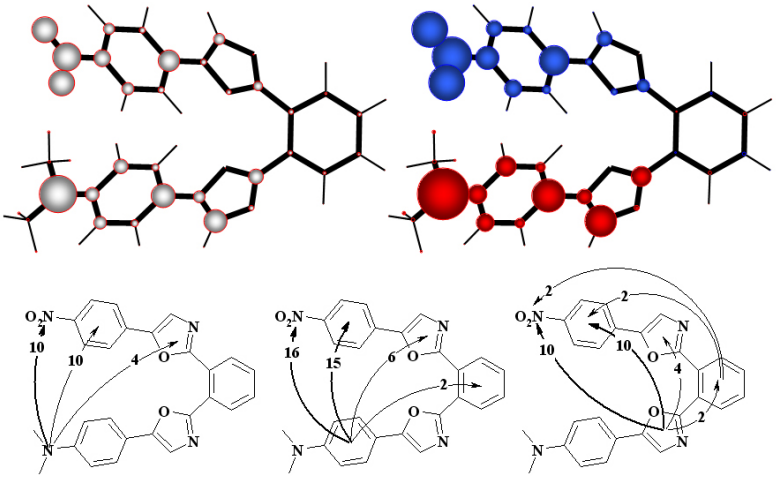

Figure 1. The ESS-analysis applied to the long-wavelength electronic transition in the absorption spectra of compound I (ground state optimized molecular geometry): localization of the electronic excitation (gray circles with radii proportional to localization numbers [27]), net charge changes (blue circles for increase of the electronic density, red – for increase of the positive charge) and arrow diagrams showing the main pathways for the electronic density movement at the electronic excitation S_0-S_1 (charge transfer indices [27]).

quartz cells. Quinine bisulfate in 0.5 M aqueous sulfuric acid served as quantum yield reference standard (φ_f = 0.546 [22]). Quadratic refraction indices quantum yield correction was implied [1-3].

Fluorescence lifetimes were measured on the nanosecond single photon counting spectrometer described elsewhere [16], decay curves were deconvoluted using non-linear least squares method [23]. Rate constants of primary photophysical photoprocesses - radiative (k_f) and radiationless (k_d) decay were calculated on the background of the experimental quantum yields and fluorescence lifetimes: $k_f = \varphi_f / \tau_f$ and $k_d = (1-\varphi_f) / \tau_f$ [1-3].

2.3. Quantum-chemical modeling

Quantum-chemical calculations were conducted by the following program packages: Gaussian-03, release E.01 [24] (for the ground state molecular structure optimization in DFT scheme *b3lyp/cc-pvdz* [25,26]), Gamess US [27] version R1 (for the excited state optimization in TDDFT scheme *TD/b3lyp/cc-pvdz*), Gaussian-09, release B.01 [28] (for the ground and excited state optimization in DFT/TDDFT scheme *TD/M06-2X/cc-pvdz* [29]) and NWChem version 5.1 [30] (equipped with special module for ESSA, "Excited State Structural Analysis", [31] - for the electronic spectra calculation and analysis).

3. Results and discussion

The title compounds contain both the most efficient neutral electron donor (N,N-dialkylamino) and electron acceptor groups (nitro) in *para*-positions of the terminal benzene rings. This allows for increased intramolecular donor-acceptor interactions in their molecules at the electronic excitation. In addition to the excited state planarization typical to the sterically hindered molecules of the *ortho*-POPOP analogs, the induced solvatochromic effects should further enlarge their abnormally high Stokes shifts observed even for the unsubstituted representatives of the investigated series [12-21].

The intramolecular electron density redistribution in the molecules of dimethylamino/nitro substituted *ortho*-POPOPs was analyzed with the ESSA approach [27], which is a generalization of the earlier scheme initially elaborated for the π-electronic calculations methods in the mid- 1970s [32]. The electronic excitation localization indices (L_i) help to elucidate the functional groups and structural fragments of the studied molecules participating in the electronic transitions. Charge transfer indices (I_{ij}) show the details of the electronic density redistribution between the atoms and more complicated fragments of the whole molecule displaying the source and destination groups participating in it. These indices are much more informative in comparison to the traditional "charge changes" in Δq format, which reflect only the final result of the intramolecular electric charge redistribution at the electronic excitation.

Applying ESSA to the S_0-S_1 electronic transition of compound **I** gives the results presented in Fig. 1. The discussed molecule is non-planar like the most of the *ortho*-analogs of POPOP: the *b3lyp/cc-pvdz* calculated angles between the oxazole cycle planes and the central benzene ring is near 29-30º. No spatial asymmetry typical to this class of organic molecules in the crystalline state and qualitatively reproduced for them by the most of semiempirical methods [12-21], was detected with DFT modeling. Moreover, such a result was unexpected for the molecule with donor and acceptor substituents, which themselves could be the reason of the electronic density distribution asymmetry.

The long-wavelength electronic transition in the absorption spectrum of **I** (calculated in TDDFT for the ground state molecular geometry) is localized mainly on the terminal benzene rings and substituents introduced in them. Participation of the heterocycles is much lower, while the central benzene ring seemingly does not take part in the electronic excitation. The charge changes look similar to L_i, however in this case the participation of the substituents is a little more prominent.

The electron density redistribution pathways (I_{ij}) analysis allows to conclude that the most important among them is the direct exchange between the donor and acceptor substituents and their neighboring benzene rings. The oxazole cycles and central benzene ring play the role of the bridge groups; their involvement in the general redistribution of the electronic density is auxiliary.

All these results allow for the classification of the S_0-S_1 electronic transition in **I** molecule as the classical intramolecular charge transfer one. Indeed, the calculated dipole moment of the discussed molecule in its lowest singlet Frank-Condon excited state exceeds that of the ground state on 26 D.

All the synthesized donor-acceptor substituted *ortho*-analogs of POPOP are characterized by substantial sensitivity to the polar nature of their environment: the fluorescence color changes from green in the low polar octane to the red in solvents of intermediate polarity (1,4-dioxane, ethyl acetate). However, fluorescence intensity of the investigated compounds decreases with solvent polarity down to complete disappearance in acetonitrile or DMF: generally, no emission lower than 14000 cm^{-1} was observed for the investigated compounds (Table 1, Fig. 2).

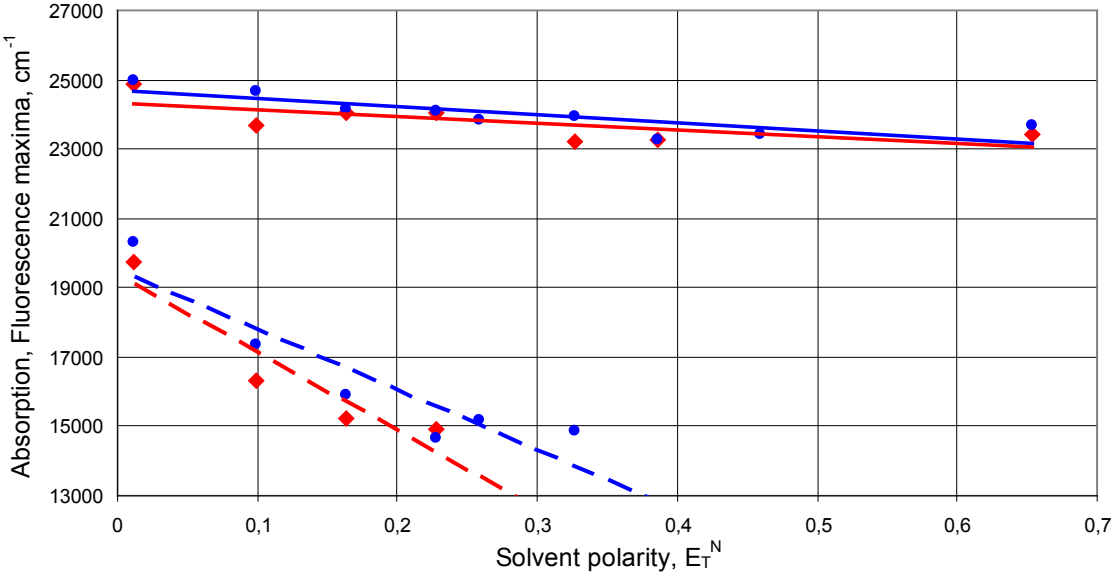

Figure 2. Solvatochromic behavior of compounds I (red lines: solid - absorption, dashed - fluorescence) and III (blue lines) presented *versus* the Reichardt solvent polarity function E_T^N [33].

The analogous tendency is typical to various organic dialkylamino-substituted molecules with strong intramolecular donor-acceptor interactions, for which the fluorescence quenching in polar and proton donor solvents was often observed, for example, see [34-39]. The probable reason for such behavior could be the specific excited state relaxation process leading to the formation of TICT (Twisted Intramolecular Charge Transfer) states [40-43], emissive for only a limited number of rather small organic molecules like the classical dimethylamino-benzonitrile, DMABN, [36,44] and dimethylamino substituted pyridines [45,46]. In most cases the structural fixation of the dialkylamino-group by the alkyl chains resulted in prohibition of intramolecular twisting and made fluorescence quenching hardly possible [36].

An alternative reason for the decrease of fluorescent ability in the highly polar surrounding could be the critically close approaching the energy of the structurally and solvent relaxed S_1* excited state to the ground state. This leads to an increase of the rate of internal conversion S_1*-S_0 in the framework of the *Energy gap law* [47-49].

To make the grounded choice between these two possible mechanisms of solvent polarity induced fluorescence quenching in the series of the investigated *ortho*-analogs of POPOP we have specially synthesized the compound **III** with the saturated alkyl bridge rigidly fixing its electron donor center, alkylamino-group, in the plane of the neighboring benzene ring. This circumstance excludes the possibility of alkylated amino-group internal rotation thus making formation of TICT states impossible [36]. However, the discussed structural modification could influence not only the conformation, but also electronic effects of such a substituent. Thus, we performed preliminary quantum-chemical modeling, aimed to outline the difference between such structurally fixed alkylamino group introduced in molecule **III** and dialkylamino groups (compounds **I**,**II**). The results of this modeling are presented in the Table 2. The simple systems containing the discussed substituents, benzene ring and electron accepting nitro-group were examined with modeling in the *b3lyp/cc-pvdz* and *TD/b3lyp/cc-pvdz* schemes for the ground and lowest singlet excited states, respectively.

The pyramidalization degree of alkylated amino-group was estimated as a sum of three valence angles formed by its nitrogen atom. The selected DFT schemes (*b3lyp/cc-pvdz*) optimal to predict electronic spectra [27] seems to slightly overestimate conjugation effects, thus no substantial pyramidality was found for dialkylamino group at our modeling. The recently developed "universal" Minnesota DFT functionals [29] qualitatively gave the same results.

The space lability of the trimethylene chain forming the partially unsaturated six-membered nitrogen heterocycle leads to the most energetically favorable chair-like conformation of the latter. This resulted in substantial general deplanarization of the corresponding model molecules and pyramidalization of their nitrogen atoms accompanied by slight increase of $N\text{-}C_{(Ar)}$ interatomic distances in the model molecules **C**, **D** in

Table 1. Spectral and photophysical properties of the dialkylamino/nitro substituted ortho-analogs of POPOP (I-III) in solvents of different polarity.

Solvent, E_T^N [29]	ν_a, cm^{-1}	λ_a, nm	ν_f, cm^{-1}	λ_f, nm	$\Delta\nu_{ST}$, cm^{-1}	φ_f	τ_f, ns	$k_f \times 10^8$, s^{-1}	$k_d \times 10^8$, s^{-1}
	1-(5-[4-N,N-dimethylamionophenyl]-2-oxazolyl)-2-(5-[4-nitrophenyl]-2-oxazolyl)-benzene (I)								
Octane, 0.012	24860	402	19740	507	5120	0.25	1.65	1.50	4.56
Toluene, 0.099	23700	422	16340	612	7360	0.22	2.39	0.91	3.28
1,4-Dioxane, 0.164	24040	416	15220	657	8820	0.07	1.26	0.54	7.40
Ethyl Acetate, 0.228	24040	416	14900	671	9140	0.001	-	-	-
1,2-Dichloroethane, 0.327	23240	430	-	-	-	-	-	-	-
DMF, 0.386	23280	430	-	-	-	-	-	-	-
Ethyl Alcohol, 0.654	23440	427	-	-	-	-	-	-	-
	1-(5-[4-N,N-dimethylamionophenyl]-1,3,4-oxadiazol-2-yl)-2-(5-[4-nitrophenyl]-2-oxazolyl)-benzene (II)								
Octane, 0.012	28740	348	20900	478	7840	0.10	1.29	0.80	6.95
Toluene, 0.099	26440	378	17820	561	8620	0.08	2.33	0.36	3.93
1,4-Dioxane, 0.164	27380	365	16940	591	10440	0.065	2.06	0.31	4.54
Ethyl Acetate, 0.228	27140	368	14980	667	12160	-	0.53	-	-
1,2-Dichloroethane, 0.327	25980	385	15220	657	10760	0.07	-	-	-
DMF, 0.386	26400	379	-	-	-	-	-	-	-
Acetonitrile, 0.460	26720	374	-	-	-	-	-	-	-
Ethyl Alcohol, 0.654	27520	363	-	-	-	-	-	-	-
	6-(2-{2-[5-(4-nitrophenyl)-1,3-oxazol-2-yl]phenyl}-1,3-oxazol-5-yl)-1,2,3,4-tetrahydroquinoline (III)								
Octane, 0.012	24960	401	20320	492	4640	0.14	3.55	0.39	2.42
Toluene, 0.099	24680	405	17360	587	7320	0.12	4.11	0.29	2.14
1,4-Dioxane, 0.164	24160	414	15920	628	8024	0.05	3.30	0.15	2.88
Ethyl Acetate, 0.228	24120	415	14660	682	6420	0.006	4.28	0.001	2.32
Chloroform, 0.259	23840	419	15200	658	8640	0.01	4.04	0.02	2.45
1,2-Dichloroethane, 0.327	23920	418	14880	672	8340	0.02	3.22	0.06	3.04
DMF, 0.386	23280	430	-	-	-	-	-	-	-
Acetonitrile, 0.460	23420	427	-	-	-	-	-	-	-
Ethyl Alcohol, 0.654	23660	423	-	-	-	-	-	-	-

Table 2. Quantum-chemical modeling of the space structure and electronic effects of the trimethylene chain fixed alkylamino group.

Calculated characteristics	Model molecules			
	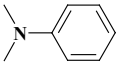	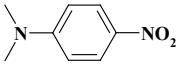		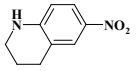
	A	**B**	**C**	**D**
Nitrogen atom pyramidalization, S_0 state	360°	360°	348°	357°
Nitrogen atom pyramidalization, S_1 state	360°	360°	359°	354°
r_{C-N}, S_0 state	1.386 Å	1.374 Å	1.397 Å	1.376 Å
r_{C-N}, S_1 state	1.423 Å	1.381 Å	1.388 Å	1.385 Å
Electronic transition S_0 - S_1	274 nm	315 nm	273 nm	323 nm
Charge transfer at the electronic transition S_0 - S_1	0.431	0.603	0.351	0.430
$\Delta\mu$ at the electronic transition S_0 - S_1	6.1 D	15.0 D	4.8 D	10.2 D

comparison with that of the **A**, **B** molecules. Introduction of the strong electron accepting nitro group smoothes this effect, however does not eliminate it entirely.

The above results reveal deterioration of the conjugation between the benzene ring and the amino group nitrogen atom at its space fixation with the alkyl chain. The tendency for hypsochromic shifts in the electronic absorption spectra and decrease of the charge transfer at the electronic excitation from the alkylamino-substituents towards the rest of the molecule followed from the above discussed circumstances.

In the structurally relaxed electronically excited state the enforced mesomeric effects dominate over the steric ones: the pyramidality of the nitrogen atoms decreases, making the model molecules more planar and more polar than in the ground state.

The above results reveal that the structural fixing of amino group with trimethylene chain leads to the disturbance of coplanarity of this substituent with the neighboring benzene ring and a decrease in the conjugation between the nitrogen atom unshared electron pair with the aromatic π-system. This also leads to the decrease of the electron donor ability of such a structurally fixed substituent, lowering the intensity of intramolecular charge transfer, short-wavelength shifts in the electronic absorption spectra and a decrease in the sensitivity of the spectral parameters to the polar influence of the environment. According to our modeling, the outlined tendencies were partially compensated by the excited state structural relaxation, thus the hypsochromic effects should be less expected in the fluorescence emission spectra.

The fact that spatial fixation of amino-group in the molecule of compound **III** could not prevent the polarity induced fluorescence quenching allows us to conclude that TICT state formation is not the main reason for the decrease of fluorescent ability in the investigated series of donor-acceptor substituted molecules. Probably, the energy gap lowering between the structurally and solvent relaxed electronically excited state and the corresponding ground state plays the key role in the dramatic decrease of fluorescence quantum yields in the studied series of the *ortho*-analogs of POPOP, in the analogy to the cases described, for example in [50-53].

However, there exists another possible hypothesis, which does not contradict the above declared Energy gap regulated fluorescence quenching in polar solvents. Systematic decrease of the experimentally estimated fluorescence emission rate constants (Table 1) and our quantum-chemical modeling of the excited state structurally relaxed conformation of the donor-acceptor substituted *ortho*-POPOP indirectly pointed to this possibility.

The quantum-chemical calculation of the structurally relaxed excited **I** molecule was conducted in the TDDFT scheme. The final "relaxed" molecular structure and the electron density redistribution in the ESSA approach are shown in the Fig. 3. It is considered, that the *b3lyp* functional is not the best one for calculation of the systems with intramolecular charge transfer [54] (it underestimates the energy yet gives, at the same time, reasonable prediction of molecular geometry), that is why we have recalculated the optimized excited state geometry also in the Truhlar's *M06-2x* [29] functional, generally showing much better results in predicting highly polar excited states [55,56]. Indeed, the *b3lyp*-calculated excited state energy was quite underestimated, however, the optimized *b3lyp* and *M06-2x* molecular geometries were practically the same. Thus, we could make several conclusions based on our TDDFT calculations. In the lowest singlet excited state of **I** the planes of the terminal benzene rings are nearly parallel with minimal distance between them close to the mean thickness of the aromatic cycle. Donor and

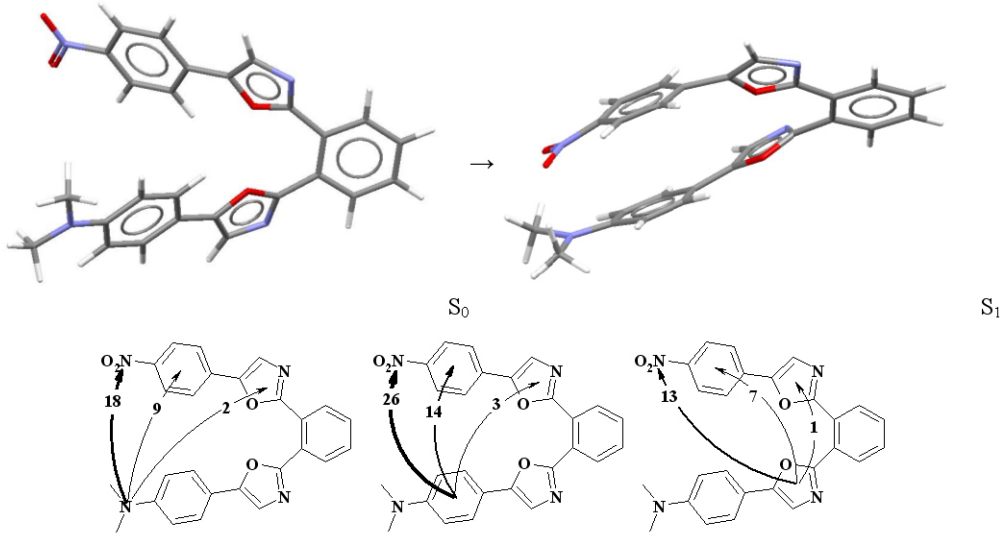

Figure 3. Ground (*b3lyp/cc-pvdz*) and excited state (*TD/b3lyp/cc-pvdz*) optimized molecular geometry of compound I and the electron density redistribution at electronic transition S_0-S_1 in the latter (ESS-analysis).

acceptor substituents are on the minimal distance one from another reflecting their significant electrostatic attraction resulting from the excited state intramolecular charge transfer. Generally, the excited state optimized structure of **I** looks like intramolecular exciplex with substantial stacking interaction of the terminal benzene rings.

The ESSA approach confirmed the increase of the intramolecular donor-acceptor interactions: charge transfer between the most important moieties intensifies significantly in the structurally relaxed lowest excited singlet state of **I**. At the same time, difference in the ground and excited state dipole moments was lower in the S_1-optimized structure in comparison with that of S_0-state one ($\Delta\mu$ ~18 D and ~26 D correspondingly). This fact reflects the spatial approaching of the nitro and the dimethylamino groups, which decreases the length of the electric dipole even while increasing the difference in electric charges and thus resulting in total decrease of $\Delta\mu = \Delta q \times l$.

The calculated charge transfer indices revealed increased direct electron density redistribution between the donor and acceptor centers of the excited structurally relaxed **I** molecule: nitro and dimethylamino groups and their neighboring benzene rings. The electronic excitation localization indices also evidenced the decreased participation of the three-cycle oxazole-phenyl-oxazole bridge moiety in the formation of the lowest structurally relaxed singlet excited state of **I**.

The energy of the long-wavelength electronic transition (calculated with *m062x/cc-pvdz* scheme) lies at ~750 nm, practically on the margin of near-infrared region. The calculated transition intensity (oscillator strength) was low, reflecting the charge transfer origin of the structurally relaxed excited state. The tendency to decrease the "experimental" k_f values calculated based on fluorescence quantum yields and lifetimes observed for compounds **I-III** (Table 1) is in line with the above fact. No one should expect fluorescence emission in the case when the excited molecule radiative rate constant dramatically decreases owing to the charge transfer nature of the structurally relaxed S_1 state, at the same time as the radiationless rate constant increases following the *Energy Gap Law* at energies approaching the structurally relaxed excited and the corresponding Franck-Condon ground state.

Thus, the excited state formation of intramolecular exciplex-like conformation should be considered among the possible reasons for the polarity-induced fluorescence quenching in the series of the investigated compounds. Recently, a possibility for the intramolecular exciplexes of the sterically hindered dendrimer-like molecules composed from the residues of the oxadiazolic analogs of *ortho*-POPOP was discussed in [57].

4. Conclusions

Fluorescence ability of the newly synthesized dialkylamino-nitro substituted derivatives of *ortho*-POPOP was examined in several solvents of different polarity. The significant solvatochromic effects both in the absorption and in the emission spectra and fluorescence quenching in polar solvents are described as a result of increased intramolecular excited state donor-acceptor interactions. The observed decrease of fluorescence quantum yields

in polar surroundings was shown to be regulated by the *Energy Gap Law* rather than TICT-mechanism. Structurally relaxed excited state conformation looking like intramolecular exciplex was predicted for the studied compounds by the quantum chemical modeling.

References

[1] J.R. Lakowicz, Principles of Fluorescence Spectroscopy, 3rd edition (Springer Science + Business Media, LLC, Singapore, 2006)

[2] B. Valeur, Molecular Fluorescence (Wiley-VCH Verlag GmbH, Weinheim, 2002)

[3] C. Parker, Photoluminescence in solutions (Elsevier, Amsterdam-London-New York, 1968)

[4] M. Eichhorn, Appl. Phys. B 96, 369 (2009)

[5] S.P. Nighswander-Rempel, J. Riesz, J. Gilmore, J.P. Bothma, P. Meredith, J. Phys. Chem. B 109, 20629 (2005)

[6] C.H. Hidrovo, R.R. Brau, D.P. Hart, Appl. Opt. 43, 894 (2004)

[7] R. Sóti, É. Farkas, M. Hilbert, Zs. Farkas, I. Ketskeméty, J. Lumin. 55, 5 (1993)

[8] F. Vollmer, W. Rettig, E. Birckner, J. Fluor. 4, 65 (1994)

[9] A.O. Doroshenko, Theor. Exper. Chem. 38, 135 (2002)

[10] J.B. Birks, The Theory and Practice of Scintillation Counting (Pergamon Press, London, Macmillan, New York, 1964)

[11] B.M. Krasovitskii, B.M. Bolotin, Organic luminescent materials (VCH Publishers, Weinheim, New York, 1988)

[12] A.O. Doroshenko, L.D. Patsenker, V.N. Baumer, L.V. Chepeleva, A.V. Van'Kevich, A.V. Kirichenko, S.N. Yarmolenko, V.M. Shershukov, V.G. Mitina, O.A. Ponomaryov, Molec. Engineering 3, 353 (1994)

[13] A.O. Doroshenko, V.N. Baumer, A.V. Kirichenko, V.M. Shershukov, A.V. Tolmachev, Chem. Heterocycl. Comp. 33, 1341 (1997)

[14] A.O. Doroshenko, A.V. Kyrychenko, V.N. Baumer, A.A. Verezubova, L.M. Ptyagina, J. Molec. Struct. 524, 289 (2000)

[15] A.O. Doroshenko, V.N. Baumer, A.A. Verezubova, L.M. Ptyagina, J. Molec. Struct. 609, 29 (2002)

[16] A.O. Doroshenko, A.V. Kirichenko, V.G. Mitina, O.A. Ponomaryov, J. Photochem. Photobiol. A: Chem. 94, 15 (1996)

[17] A.V. Kirichenko, A.O. Doroshenko, V.M. Shershukov, Chem. Phys. Reports 17, 1643 (1998)

[18] A.O. Doroshenko, A.V. Kyrychenko, J. Waluk, J. Fluor. 10, 41 (2000)

[19] A.O. Doroshenko, Chem. Phys. Reports 18, 873 (1999)

[20] A.O. Doroshenko, Russ. Journ. Phys. Chem. 74, 773 (2000)

[21] A.O. Doroshenko, T.V. Sakhno, A.V. Kyrychenko, Spec. Lett. 35, 171 (2002)

[22] W.A. Melhuish, J. Phys. Chem. 65, 229 (1961)

[23] J.N. Demas, A.W. Adamson, J. Phys. Chem. 75, 2463 (1971)

[24] M.J. Frisch, G.W. Trucks, H.B. Schlegel, G.E. Scuseria, M.A. Robb, J.R. Cheeseman, J.A. Montgomery,Jr., T. Vreven, K.N. Kudin, J.C. Burant, J.M. Millam, S.S. Iyengar, J. Tomasi, V. Barone, B. Mennucci, M. Cossi, G. Scalmani, N. Rega, G.A. Petersson, H. Nakatsuji, M. Hada, M. Ehara, K. Toyota, R. Fukuda, J. Hasegawa, M. Ishida, T. Nakajima, Y. Honda, O. Kitao, H. Nakai, M. Klene, X. Li, J.E. Knox, H.P. Hratchian, J.B. Cross, V. Bakken, C. Adamo, J. Jaramillo, R. Gomperts, R.E. Stratmann, O. Yazyev, A.J. Austin, R. Cammi, C. Pomelli, J.W. Ochterski, P.Y. Ayala, K. Morokuma, G.A. Voth, P. Salvador, J.J. Dannenberg, V.G. Zakrzewski, S. Dapprich, A.D. Daniels, M.C. Strain, O. Farkas, D.K. Malick, A.D. Rabuck, K. Raghavachari, J.B. Foresman, J.V. Ortiz, Q. Cui, A.G. Baboul, S. Clifford, J. Cioslowski, B.B. Stefanov, G. Liu, A. Liashenko, P. Piskorz, I. Komaromi, R.L. Martin, D.J. Fox, T. Keith, M.A. Al-Laham, C.Y. Peng, A. Nanayakkara, M. Challacombe, P.M.W. Gill, B. Johnson, W. Chen, M.W. Wong, C. Gonzalez, J.A. Pople, Gaussian 03, Revision E.01 (Gaussian, Inc., Wallingford, CT, 2004)

[25] A.D. Becke, J. Chem. Phys. 98, 5648 (1993)

[26] D.E. Woon, T.H. Dunning, J. Chem. Phys. 98, 1358 (1993)

[27] M.W. Schmidt, K.K. Baldridge, J.A. Boatz, S.T. Elbert, M.S. Gordon, J.H. Jensen, S. Koseki, N. Matsunaga, K.A. Nguyen, S.J. Su, T.L. Windus, M. Dupuis, J.A. Montgomery, J. Comput. Chem. 14, 1347 (1993)

[28] M.J. Frisch, G.W. Trucks, H.B. Schlegel, G.E. Scuseria, M.A. Robb, J.R. Cheeseman, G. Scalmani, V. Barone, B. Mennucci, G.A. Petersson, H. Nakatsuji, M. Caricato, X. Li, H.P. Hratchian,

A.F. Izmaylov, J. Bloino, G. Zheng, J.L. Sonnenberg, M. Hada, M. Ehara, K. Toyota, R. Fukuda, J. Hasegawa, M. Ishida, T. Nakajima, Y. Honda, O. Kitao, H. Nakai, T. Vreven, J.A. Montgomery,Jr., J.E. Peralta, F. Ogliaro, M. Bearpark, J.J. Heyd, E. Brothers, K.N. Kudin, V.N. Staroverov, R. Kobayashi, J. Normand, K. Raghavachari, A. Rendell, J.C. Burant, S.S. Iyengar, J. Tomasi, M. Cossi, N. Rega, J.M. Millam, M. Klene, J.E.Knox,J.B.Cross,V.Bakken,C.Adamo,J.Jaramillo, R. Gomperts, R.E. Stratmann, O. Yazyev, A.J. Austin, R. Cammi, C. Pomelli, J.W. Ochterski, L. Martin., K. Morokuma, V.G. Zakrzewski, G.A. Voth, P. Salvador, J.J. Dannenberg, S. Dapprich, A.D. Daniels, O. Farkas, J.B. Foresman, J.V. Ortiz, J. Cioslowski, D.J. Fox, Gaussian 09, Revision A.01, (Gaussian Inc., Wallingford CT, 2009)

[29] Y. Zhao, D.G. Truhlar, Theor. Chem. Acc. 120, 215 (2008)

[30] E.J. Bylaska, W.A. de Jong, N. Govind, K. Kowalski, T.P. Straatsma, M. Valiev, D. Wang, E. Apra, T.L. Windus, J. Hammond, P. Nichols, S. Hirata, M.T. Hackler, Y. Zhao, P.-D. Fan, R.J. Harrison, M. Dupuis, D.M.A. Smith, J. Nieplocha, V. Tipparaju, M. Krishnan, Q. Wu, T. Van Voorhis, A.A. Auer, M. Nooijen, E. Brown, G. Cisneros, G.I. Fann, H. Fruchtl, J. Garza, K. Hirao, R. Kendall, J.A. Nichols, K. Tsemekhman, K. Wolinski, J. Anchell, D. Bernholdt, P. Borowski, T. Clark, D. Clerc, H. Dachsel, M. Deegan, K. Dyall, D. Elwood, E. Glendening, M. Gutowski, A. Hess, J. Jaffe, B. Johnson, J. Ju, R. Kobayashi, R. Kutteh, Z. Lin, R. Littlefield, X. Long, B. Meng, T. Nakajima, S. Niu, L. Pollack, M. Rosing, G. Sandrone, M. Stave, H. Taylor, G. Thomas, J. van Lenthe, A. Wong, Z. Zhang, NWChem, A Computational Chemistry Package for Parallel Computers, Version 5.1 (Pacific Northwest National Laboratory, Richland, Washington, USA, 2007)

[31] A.V. Luzanov, O.A. Zhikol, Int. J. Quant. Chem. 110, 902 (2010)

[32] A.V. Luzanov, Russ. Chem. Rev. 49, 1033 (1980)

[33] C. Reichardt, Chem. Rev. 94, 2319 (1994)

[34] I.A.Z. Al-Ansari, J. Phys. Org. Chem. 10, 687 (1997)

[35] D. Yuan, R.G. Brown, J. Phys. Chem. A 101, 3461 (1997)

[36] A.B.J. Parusel, W. Nowak, S. Grimme, G. Köhler, J. Phys. Chem. A 102, 7149 (1998)

[37] L. Biczók, T. Bérces, H. Inoue, J. Phys. Chem. A 103, 3837 (1999)

[38] F. Gao, H-R. Li, Y-y. Yang, Dyes Pigm. 47, 231 (2000)

[39] K. Rurack, J.L. Bricks, G. Reck, R. Radeglia, U. Resch-Genger, J. Phys. Chem. A 104, 3087 (2000)

[40] Z.R. Grabowski, K. Rotkiewicz, A. Siemiarczuk, D.J. Cowley, W. Baumann, Nouv. J. Chim. 3, 443 (1979)

[41] W. Rettig, Ang. Chem. Intl. Ed. Engl. 25, 971 (1986)

[42] E. Lippert, W. Rettig, V. Bonacic-Koutecky, F. Heisel, J.A. Miehe, Adv. Chem. Phys. 68, 1 (1987)

[43] Z.R. Grabowski, K. Rotkiewicz, W. Rettig, Chem. Rev. 103, 3899 (2003)

[44] G. Wermuth, W. Rettig, E. Lippert, Ber. Bunsenges. phys. Chem. 85, 64 (1981)

[45] J. Herbich, J. Waluk, Chem. Phys. 188, 247 (1994)

[46] S. Mishina, S. Takayanagi, M. Nakata, J. Otsuki, K. Araki, J. Photochem. Photobiol. A: Chem. 141, 153 (2001)

[47] P. Avouris, W.M. Gelbart, M.A. El-Sayed, Chem. Rev. 77, 793- (1977)

[48] R. Englman, J. Jortner, Mol. Phys. 18, 145 (1970)

[49] W. Siebrand, J. Chem. Phys. 55, 5843 (1974)

[50] H. Fidder, M. Rini, E.T.J. Nibbering, J. Amer. Chem. Soc. 126, 3789 (2004)

[51] A.O. Doroshenko, M.D. Bilokin, V.G. Pivovarenko, J. Photochem. Photobiol. A: Chem. 163, 95 (2004)

[52] R.J. Willemse, D. Theodori, J.W. Verhoeven, A.M. Brouwer, Photochem. Photobiol. Sci. 2, 1134 (2003)

[53] A.O. Doroshenko, V.G. Pivovarenko, J. Photochem. Photobiol. A: Chem. 156, 55 (2003)

[54] A. Dreuw, M. Head-Gordon, Chem. Rev. 105, 4009 (2005)

[55] Y. Zhao, D.G. Truhlar, Chem. Phys. Lett. 502, 1 (2011)

[56] X. Liu, D. Yang, H. Ju, F. Teng, Y. Hou, Z. Lou, Chem. Phys. Lett. 503, 75 (2011)

[57] C-C. Yang, C-J. Hsu, P-T. Chou, H.C. Cheng, Y.O. Su, M-K. Leung, J. Phys. Chem. B 114, 756 (2010)